Int J Adv Manuf Technol (2015) 77:1811–1818
DOI 10.1007/s00170-014-6578-9

ORIGINAL ARTICLE

Investigation of the taper of kerfs cut in steels by AWJ

Libor M. Hlaváč · Irena M. Hlaváčová · Vladan Geryk · Štefan Plančár

Received: 10 April 2014 / Accepted: 9 November 2014 / Published online: 19 November 2014

Abstract The abrasive water jet (AWJ) taper inside the cut material is one of the characteristic phenomena of the AWJ cutting. The taper, together with a retardation of the jet inside the kerf, causes deformation of workpieces, especially in corners and curvatures. Some deviations of the side walls from the plains perpendicular to the material surface can be observed and measured even in the straight line parts of trajectories. This paper is aimed at experimental research of this phenomenon on steels because precision cutting of stainless and hard steels with thicknesses over 10 mm is a serious problem in practice, and the AWJ cutting can solve this problem quite well. The experiments were performed on three sets of steel plates with thicknesses close to 30 mm. The steels of the first and the second set were identical (1.2379, 1.3343, 1.4307, 1.4404 and 1.4845). The steels of the first set were cut in their normal states, and the steels of the second set were subjected to cooling in the liquid nitrogen prior to cutting (marked 1.abcd/N). The third set of samples consisted of steels with very different composition and brittle/ductile behaviour cut in their normal states (1.0036, 1.2767, 1.3379, 1.7225 and 1.7733). The model for calculation of the limit traverse speed from both the jet parameters and material properties has been used for determination of the proper traverse speed scale. The widths of the cuts were measured both on the top and on the bottom of the slots. The difference between these widths has been used for evaluation of the inclination angle, i.e. the wall deviation from the plane perpendicular to the material surface, referred also as the taper. This angle can be used for determination of the tilting angle for compensation of the negative influence on workpiece. The influence of brittle/ductile behaviour and the influence of cooling in liquid nitrogen have been tried to find out. The results were also compared with the theoretical relationship between traverse speed and inclination angle (the taper) on steels presented as a result of previous investigations in scientific articles. The difference between the inlet and the outlet width of kerf made by AWJ in tested steels ranges from 5.2 to 35.4 % for the traverse speed of 5 mm min^{-1} and from 25.5 to 44.9 % for the traverse speed of 50 mm min^{-1}.

Keywords Abrasive water jet · Cutting · Taper · Steel · Shape distortion

L. M. Hlaváč (✉) · I. M. Hlaváčová · V. Geryk
Faculty of Mining and Geology, Institute of Physics,
VŠB—Technical University of Ostrava, 17.listopadu 15/2172,
70833, Ostrava Poruba, Czech Republic
e-mail: libor.hlavac@vsb.cz

I. M. Hlaváčová
e-mail: irena.hlavacova@vsb.cz

V. Geryk
e-mail: vladan.g@centrum.cz

Š. Plančár
Watting, s.r.o., Budovateľská 38, 080 01 Prešov, Slovak Republic
e-mail: watting@watting.sk

Nomenclature

α	coefficient of water jet velocity loss in interaction with material
α_e	experimentally determined coefficient of abrasive water jet velocity loss in interaction with material
γ	compressibility of liquid (water) (Pa^{-1})
γ_o	liquid (water) compressibility factor ($1-\gamma p_o$)
η	liquid (water) dynamic viscosity (Pa s)
θ	angle between impinging jet axis and tangent to the striation curve at depth h (°)
θ_{lim}	absolute value of angle between impinging jet axis and tangent to the striation curve at depth h_{lim} (°)

μ_o liquid (water) nozzle discharge coefficient
ν Poisson's ratio
ξ_j attenuation coefficient of abrasive jet in the environment between the focussing tube outlet and the material surface (m^{-1})
ρ density of liquid (water) (kg m^{-3})
ρ_a density of abrasive material (kg m^{-3})
ρ_j density of abrasive jet (conversion to homogeneous liquid) (kg m^{-3})
ρ_m density of material being machined (kg m^{-3})
σ trailback (m)
σ_m strength of material being machined (Pa)
τ shear stress (Pa)
φ inclination angle of the cut walls (°)
φ_{lim} inclination angle of the cut walls in the bottom for limit cutting (°)
χ coefficient of jet broadening in relation to outlet orifice size
a_n mean size of abrasive particles formed in the mixing process (m)
a_m mean size of particles (elements) of material—grains or their chips (m)
a_o mean size of abrasive particles entering the mixing process (m)
c sound velocity inside the abrasive material (m s^{-1})
c_o sound velocity inside liquid used for preparation of abrasive liquid jet (usually water) (m s^{-1})
C_1 coefficient modifying abrasive jet velocity in relation to the quantity of abrasive input
C_2 coefficient modifying abrasive jet velocity in relation to the ratio between focussing tube diameter and average abrasive particle size resulting from the mixing process
C_3 coefficient modifying abrasive jet velocity in relation to the friction inside the focussing tube and the ratio between the length of the actual focussing tube and the length of the tube considered to be a standard
C_4 coefficient modifying abrasive jet velocity in relation to focussing tube clearness
C_A coefficient modifying abrasive water jet performance in relation to the changing content of abrasive below so-called saturation level (above this level, the jet performance increases no more and $C_A=1$)
C_D abrasive particle drag coefficient inside liquid used for preparation of abrasive liquid jet (usually water)
C_Q coefficient modifying the limit depth of cut or limit traverse speed to the values assuring selected quality even at the worse part of the cutting wall
d_o diameter of the water nozzle (m)
E_P specific surface energy of abrasive material (J)
$\overline{F}$ average force breaking material elements (N)
H material thickness (m)
I force momentum (kg m s^{-1})
L stand-off distance (distance between the exit of the focussing tube and the material surface) (m)
K material hardness (N m^{-2})
p_j pressure obtained from Bernoulli's equation for *liquid* with density and velocity of *abrasive jet* (Pa)
p_m momentum of a broken material element (kg m s^{-1})
p_o pressure of liquid before liquid nozzle (Pa)
P cut taper (m)
q linear shit of the angle (°)
q_a abrasive mass flow rate (kg s^{-1})
q_w water mass flow rate (kg s^{-1})
R_1 radius of the trajectory curvature on the inlet surface of the cut (m)
R_2 radius of the trajectory curvature on the outlet surface of the cut (m)
S_P ratio between the quantity of non-damaged grains (i.e. not containing defects) and the total quantity of grains in the supplied abrasive material
t time (s)
t_i interaction time (s)
v_a abrasive jet speed after the mixing process (m s^{-1})
v_i water jet speed before the mixing process (m s^{-1})
v_m material speed after the interaction process (m s^{-1})
v_L water jet speed at distance L from the nozzle outlet (m s^{-1})
v_P traverse speed of jet trace on the material surface (m s^{-1})
v_{Pmin} minimum traverse speed of cutting—correction for the zero traverse rate (the value should be equal to the average mean size of the abrasive particles after the mixing process per minute, i.e. $v_{Pmin}=a_n/60$) (m s^{-1})
v_{Plim} limit traverse speed of jet trace on the material surface calculated for the thickness H (m s^{-1})
v_{PQ} traverse speed of jet trace on the material surface ensuring selected quality of the cutting wall on the whole thickness H of material (m s^{-1})
V water jet volume entering the interaction process (m^3)
V_m volume of material exiting the interaction process (m^3)

1 Introduction

Abrasive water jet (AWJ) has been investigated for years, but still there are many phenomena to be better described, explained and used for higher precision of material machining. The first models prepared for AWJ description and evaluation were presented by Hashish [1] and Zeng and Kim [2]. The next investigations were focused also on the machining processes [3, 4] and improvement of the cutting quantity and quality [5–8]. Some microscopic models [9], macroscopic models [10] and phenomenological description [11] were also

prepared. However, a lot of work remains to be done to develop a sufficiently complex system of equations inherently including the AWJ origin, propagation in the environment and its interaction with materials. Meanwhile, the regression models are still produced [12, 13] in spite of their limited relevance.

One of the theoretical approaches, with a potential to cover many sub-processes and parameter combinations, is based on the laws of conservation. It was presented in the early 1990s [14], and since then, this model has been continually enhanced, improved and updated [5, 11]. This paper is aimed at the experimental research of the taper formation during AWJ cutting. Then, the theoretical equations for determination of the taper from the respective cutting factors and parameters are submitted.

The problem of the trailback and the taper has been studied experimentally also by Hashish [15] or Ma and Deam [16]. The approach presented in this paper is based on the determination of the limit values of either material thickness or traverse speed from the model presented in [5] and [11]. Further miniaturisation of abrasive water jets requires a significant improvement in the instruments for prediction and control of production quality because the efficiency and quality of AWJ cutting depends on many material properties. That is why much more experimental and theoretical studies of interactions are necessary to develop abrasive water jet machining tools for widths of cut below 0.1 mm, i.e. for AWJ micro-machining. Therefore, some recent papers are dealing with the taper formation during the abrasive water jet cutting process [17, 18] as well as with the influence of metal ductility in the AWJ-based processes, e.g. milling [19], or simulations of AWJ machining [20].

The up-to-date experiments on metals show the direct relation between increasing ductility and decreasing declination angle for fixed cutting parameters. This statement correlates with the principal conclusions drawn from prior models based on descriptions of particle behaviour during material wear [1, 2, 9, 21]. Together with further research in abrasive disintegration during the mixing process [22, 23], the presented experimental data and theoretical investigation yield a very interesting base for a complex description of the AWJ generation, its progress outside the focussing tube and disintegrating influence on material. Research activities are supported by investigation aimed at surface quality and vibrations caused by mixing process [24, 25].

2 Theoretical base

The depths of water jet penetration into material has been described by energy conservation law in the system liquid jet–solid-state material and conservation law of the momentum between liquid and chipping material [14]

$$\frac{1}{2}\rho V v_L^2 = \frac{1}{2}\rho V \alpha^2 v_L^2 + \frac{1}{2}\rho_\mathrm{m} V_\mathrm{m} v_\mathrm{m}^2 + \int_0^h \sigma_\mathrm{m} \chi d_\mathrm{o} v_P t_\mathrm{i} \mathrm{d}x \tag{1}$$

$$\rho v_L \mathrm{dV} = \rho \alpha v_L \mathrm{dV} + \overline{F}\mathrm{d}t \tag{2}$$

The subsequent equations, describing the impulse of force and the equivalent change of the momentum of the breaking material, have been used for evaluation of the time element dt characterising the material chipping

$$\mathrm{d}I = \frac{1}{2}\tau\pi a_\mathrm{m}^2 \mathrm{d}t \tag{3}$$

$$\Delta p_\mathrm{m} = \rho_\mathrm{m}\frac{\pi K a_\mathrm{m}}{16\nu\eta}\mathrm{d}V = \mathrm{d}I \tag{4}$$

Then, the abrasive particle size change [23] and respective velocity acceleration during the mixing process are expressed throughout these two equations, respectively [5]:

$$a_n = \frac{a_\mathrm{o}}{1 + \dfrac{C_\mathrm{D}\pi d_\mathrm{o}^2 \mu_\mathrm{o}^2 p_\mathrm{o}^2 \gamma_\mathrm{o}^2}{24\rho E_\mathrm{P} a_\mathrm{o} c_\mathrm{o} c}} \tag{5}$$

$$v_\mathrm{a} = C_1 C_2 C_3 C_4 v_\mathrm{i}\frac{q_\mathrm{w}}{q_\mathrm{w} + q_\mathrm{a}} \tag{6}$$

The set of equations for calculation of the limit depth of penetration of the abrasive water jet into the material has been derived from the above-presented equations using description of the jet as the one formed by hypothetic pure liquid with density and pressure recalculated from the abrasive water jet parameters [5]:

$$\rho_\mathrm{j} = \frac{4\rho_\mathrm{a}(q_\mathrm{w} + q_\mathrm{a})}{\pi\rho_\mathrm{a} v_\mathrm{i} d_\mathrm{o}^2 + 4q_\mathrm{a}} \tag{7}$$

$$p_\mathrm{j} = \frac{1}{2}\rho_\mathrm{j} v_\mathrm{a}^2 \tag{8}$$

Because the AWJ cutting process is usually performed for a given material thickness, the equation for calculation of the limit traverse speed v_Plim respective to the selected material

thickness H (for the respective material properties and the set cutting parameters) has been derived [5]. Its final form has been presented, e.g. in [26]:

$$v_{\mathrm{Plim}} = \left[\frac{C_{\mathrm{A}}\ S_{\mathrm{p}}\ \pi\ d_{\mathrm{o}}\ \sqrt{2\rho_{\mathrm{j}} p_{\mathrm{j}}^{3}\ e^{-5\xi_{\mathrm{j}} L}}\ \left(1 - \alpha_{\mathrm{e}}^{2}\right)}{8\ H\ \left(p_{\mathrm{j}}\rho_{\mathrm{m}}\alpha_{\mathrm{e}}^{2}\ e^{-2\xi_{\mathrm{j}} L} + \sigma_{\mathrm{m}}\rho_{\mathrm{j}}\right)} \right]^{\frac{2}{3}} - v_{\mathrm{Pmin}} \tag{9}$$

The traverse speed value for the selected quality can be determined from the five-step kerf evolution process described in [11]:

$$v_{\mathrm{PQ}} = C_{\mathrm{Q}} v_{\mathrm{Plim}} \tag{10}$$

Similarly to the declination angle of the jet axis inside the cutting kerf [11], being in a direct relation with the respective wall quality at a certain depth, the inclination angle of the cut wall can be introduced. It is supposed that it is in a direct correlation with the taper and cut walls convergence [27]. The inclination angle φ is measured between the impinging jet axis and the tangent to the cut wall in the plane comprising jet axis and perpendicular to the plane determined by the jet axis and the traverse speed vector at the selected depth. It has been assessed from experiments that, for the depth h in the material, the inclination angle can be calculated from the equation:

$$\varphi = \varphi_{\mathrm{lim}} \left(\frac{h}{h_{\mathrm{lim}}} \right)^{\frac{2}{5}} + q \tag{11}$$

It is supposed that the linear shift q of the function is strongly related to both the material and the cutting parameters and so it decides about the shape of the cross-section profile of the kerf. The shift of the cut sidewall towards the jet axis caused by jet convergence inside the cut is marked P (see Fig. 1 similar to the one presented in [26]). For very low traverse speeds, the sidewalls can be inclined in the opposite side, i.e. from the jet axis, because the jet is diverging instead of converging inside the kerf (P value is negative).

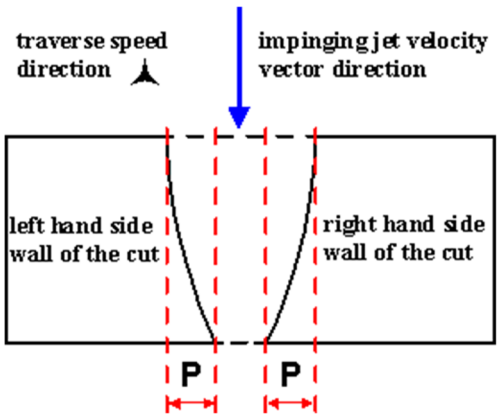

Fig. 1 Sketch of the geometrical finding of the parameter P necessary for determination of the shape deviation—cut side wall inclination

Some investigation of the jet convergence (and divergence) was presented already [27]. This time, the steel samples with both bigger thickness and higher cutting resistance have been investigated.

3 Experiments

All presented experiments were performed on the standard x–y table used for water jetting in the company Watting, Ltd. The following parameters were kept invariable for all cuts:

Pressure inside the pumping system	360 MPa
Water orifice diameter	0.25 mm
Stand-off distance	3–6 mm
Focussing tube diameter	1.02 mm
Focussing tube length	76 mm
Abrasive mass flow rate	300 g/min
Abrasive material average grain size	0.250 mm (80 mesh)
Abrasive material type	Indian garnet
Angle of impact	0 rad (0 °)
Material thickness	30 mm

The range of the stand-off distance is caused by slight differences in thicknesses of cut steel plates. All the cuts were linear and they were performed from the drilled holes prepared before the first cut (Fig. 2). Two different methods of kerf widths evaluation were applied. The first one was direct measurement—the kerf width was measured by means of the digital Vernier calliper in ten randomly selected points along the slot length both on the inlet and on the outlet surface of cut material. The second one was area averaging—the area of the slot opening on the material surface (either inlet or outlet one) was divided by the slot length. This measurement was done using software for photo processing. The combined uncertainty of both processes was almost identical, about 8 %. Therefore, it can be concluded that presented average results are measured with the uncertainty ±8 %.

The first experiments were performed on 15 materials with (supposed) different properties, regarding the composition or thermal treatment of material. All samples were approximately 30 mm thick; therefore, the limit depth of cut in these materials should be slightly above 40 mm for selected cutting parameters. Based on this knowledge, the traverse speed scales 10, 20, 30, 40 and 50 mm min^{-1} were chosen for the experiment. Five samples (steels 1.4307 and 1.4404 cooled in liquid nitrogen and three non-cooled steels 1.0036, 1.2767 and 1.7733, added later to widen the scale of properties,

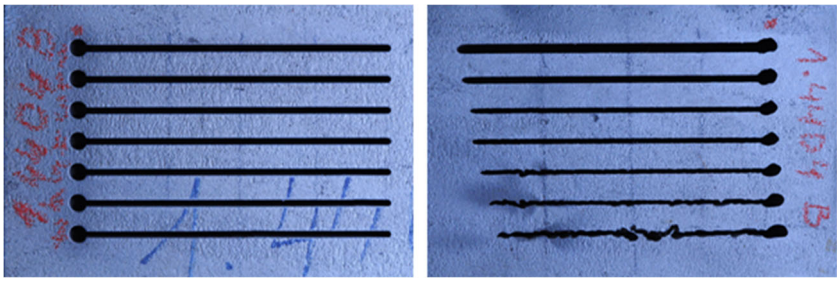

Fig. 2 Photo of slots in the steel sample: *left* inlet surface, *right* outlet surface

composition and resistance to cutting) were cut also using the traverse speeds of 5 and 15 mm min^{-1}. The respective results for the inlet and the outlet kerf widths are summarised in Tables 1 and 2 for ten non-cooled and five cooled steels (marked by /N). None of the tested steels could be cut with the traverse speed of 60 mm min^{-1} or higher at the selected thickness and AWJ cutting parameters.

All steel samples were quite well cut up to the traverse speed of 40 mm min^{-1}. Many samples were cut through only partially with the traverse speed of 50 mm min^{-1}. The stainless steels are identical with those presented in the paper reporting on the previous part of research—the investigation of roughness of the cut walls and declination angle of striations on the cut walls of the cooled steels [28].

During analyses of the experimental results presented in this paper, it has been mentioned that jet with selected parameters and traverse speed over 50 mm min^{-1} was not able to cut more brittle and harder steels in selected thickness sufficiently. Cuts performed with the traverse speed higher than the limit value (slightly above 40 mm min^{-1}) show a frayed bottom edge and highly irregular kerf width (see Fig. 2). The penetration through material is similar to a sequence of gradual piercings caused by a local increase in jet energy, when traverse speed is higher than 50 mm min^{-1}, specially in more ductile steels. On the contrary, for traverse speeds lower than 30 % of the limit value (i.e. below 10 mm min^{-1}), the penetration of the jet through material is similar to the cutting by a chop saw, and the sidewalls of the cuts are rather diverging or parallel.

4 Discussion

The analysis of the influence of the trailback and the taper in the curved parts of trajectories leads to the conclusions that the radii of the curves on the inlet surface and on the outlet surface are different for curved trajectories when all material and jet parameters are constant [26]. The inclination angle (of side walls) is usually much smaller than the declination angle (caused by jet retardation in the kerf) for most of the common cutting conditions. Nevertheless, it can substantially influence

Table 1 The results of kerf widths measurements on steels selected for experiments—inlet surface

Materials—norm DIN		Traverse speeds						
	H (mm)	5 (mm/min)	10 (mm/min)	15 (mm/min)	20 (mm/min)	30 (mm/min)	40 (mm/min)	50 (mm/min)
1.0036	30.4	1.17	1.15	1.13	1.12	1.10	1.10	1.10
1.2379	31.2	–	1.08	–	1.04	1.02	0.99	0.97
1.2379/N	31.2	–	1.03	–	1.02	1.01	1.00	0.99
1.2767	29.6	1.30	1.24	1.22	1.19	1.17	1.16	1.14
1.3343	30.8	–	1.13	–	1.09	1.04	1.01	1.00
1.3343/N	30.8	–	1.07	–	1.01	0.99	0.98	0.97
1.3379	31.6	–	1.09	–	1.07	1.05	1.02	0.98
1.4307	30.6	–	1.14	–	1.10	1.08	1.05	1.04
1.4307/N	30.6	1.07	1.02	1.01	0.98	0.93	0.88	0.84
1.4404	30.6	–	0.98	–	0.89	0.88	0.87	0.85
1.4404/N	30.6	1.15	1.11	1.02	0.99	0.97	0.96	0.95
1.4845	30.6	–	1.04	–	1.03	1.02	1.01	1.00
1.4845/N	30.6	–	1.10	–	1.06	1.05	1.04	1.03
1.7225	30.2	–	1.23	–	1.17	1.12	1.12	1.11
1.7733	30.8	1.30	1.23	1.07	1.03	1.01	0.98	0.97

Table 2 The results of kerf widths measurements on steels selected for experiments—outlet surface

Materials—norm DIN		Traverse speeds						
	H (mm)	5 (mm/min)	10 (mm/min)	15 (mm/min)	20 (mm/min)	30 (mm/min)	40 (mm/min)	50 (mm/min)
1.0036	30.4	1.584	1.302	1.154	1.054	0.922	0.806	0.606
1.2379	31.2	–	0.960	–	0.846	0.608	0.584	–
1.2379/N	31.2	–	0.952	–	0.738	0.716	0.612	–
1.2767	29.6	1.496	1.246	1.098	0.980	0.864	0.772	0.672
1.3343	30.8	–	1.032	–	0.748	0.640	0.508	–
1.3343/N	30.8	–	0.990	–	0.744	0.648	0.514	–
1.3379	31.6	–	0.958	–	0.750	0.626	0.564	–
1.4307	30.6	–	1.138	–	0.854	0.672	0.654	0.638
1.4307/N	30.6	1.270	1.090	0.912	0.846	0.728	0.644	0.626
1.4404	30.6	–	0.982	–	0.742	0.674	0.620	0.546
1.4404/N	30.6	1.518	1.158	0.838	0.738	0.712	0.686	0.580
1.4845	30.6	–	0.922	–	0.796	0.734	0.680	0.620
1.4845/N	30.6	–	1.166	–	0.866	0.726	0.640	0.600
1.7225	30.2	–	1.192	–	0.912	0.738	0.704	–
1.7733	30.8	1.368	1.122	0.942	0.810	0.678	0.588	0.566

accuracy of abrasive water jet cutting especially for thick materials, like it has been analysed in [26].

Data measured on kerfs in selected steels, cut with the parameters and variables quoted above, demonstrate interesting statements. Firstly, the kerf widths produced on the inlet surface of material are similar for all tested steels, and their values differ only about 10 % within the selected traverse speed range (see Fig. 3 or Table 1). The differences range within the frame of the measurement uncertainties for this type of experiment. Therefore, it can be stated that the kerf width on the inlet surface is almost identical for all tested materials. The small differences can be also caused by small differences in the stand-off distance caused by differences in sample thicknesses (position of the cutting head above the cutting table plane was not set up for each sample separately).

On the other hand, changes of the kerf width on the outlet surface exceed even 40 % within the selected traverse speed range for some materials (Fig. 4 or Table 2). The difference between the inlet and the outlet width of kerf cut by AWJ in five tested steels varies between values 5.2 and 35.4 % for traverse speed of 5 mm min^{-1}. The analogue difference determined for identical materials and traverse speed of 50 mm min^{-1} is varying between 25.5 and 44.9 %. The increase in this difference is small for ductile steels (up to 10 %) and huge for the brittle and resistant to wear ones (even more than 35 %). Differences caused by changes of plasticity and ductility are, therefore, more evident. Brittle steels, like 1.2379, 1.2767, 1.3343 or 1.7733, are cut worse. The influence of plasticity is presented in [29], and the influence of ductility has been mentioned in [30, 31]. The relation of the inclination angle φ to the traverse speed is expressed in Fig. 5 for steels both influenced and uninfluenced by liquid nitrogen. It can be seen that cooling of steels led to an increase in ductility (1.2379, 1.3343 or 1.4307) or to an increase in brittleness (1.4404 or 1.4845). Nevertheless, the changes differ both in character and in range and so they are not very conclusive. Therefore, few more materials not cooled in nitrogen were tested to prove differences in behaviour between ductile (1.3379 or 1.7225) and brittle steels (1.0036, 1.2767 or 1.7733). These results are graphically presented in Fig. 6. The relationship of the inclination angle on the traverse speed is more linear and steep for brittle steels (e.g. 1.0036, 1.2767, 1.3343 or 1.7733). The increase in ductility induces change of the relationship trend towards parabolic shape (1.3343/N, 1.4307/N, 1.4845/N, 1.3379 or 1.7225).

The theoretical line is calculated using Eq. 11 for these values of constants: $\varphi_{\lim}=0.9$, $q=0.42$ (see [27]). The

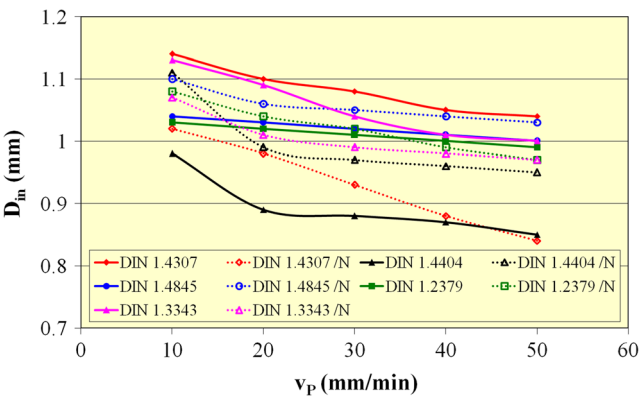

Fig. 3 Relation between the kerf widths made by AWJ on the inlet material surface and the traverse speed

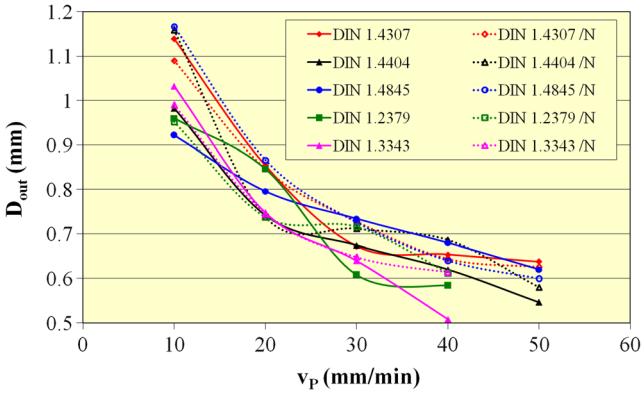

Fig. 4 Relation between the kerf widths made by AWJ on the outlet material surface and the traverse speed

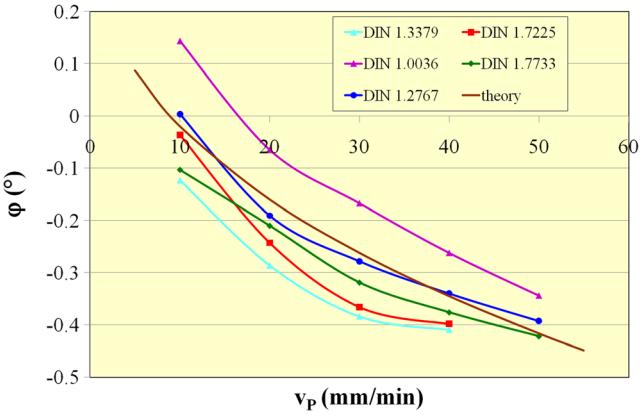

Fig. 6 Relation between the inclination angle of the cut walls made by AWJ and the traverse speed for more and less ductile non-cooled steels

correlation with experimental data is not sufficiently strong, and, therefore, it is necessary to continue this research.

Two phenomena are considered to play the decisive role in the discrepancy between the previously determined Eq. 11 (see [27]) and the contemporary results. Considering the research presented in [4, 7, 32–34], the substantially higher thicknesses of material were cut this time, and plasticity of tested stainless steels was higher as well. The higher plasticity causes a lower increase in inclination angle value with increasing traverse speed comparing with the more brittle steels. This phenomenon is well seen on the graph in Fig. 5—some of the steels exposed by liquid nitrogen (1.3343 or 1.4307) became less resistant and more ductile: the relationship between the inclination angle of the cut walls and the traverse speed is more parabolic and shifted to positive values for material cooled in nitrogen. For other steels (1.4404 and 1.4845), the effect of cooling is quite different. The relationship between the inclination angle of the cut walls and the traverse speed is more parabolic and shifted to negative values for material cooled in nitrogen. One material (1.2379) did not exhibit definite change in behaviour due to cooling in nitrogen. The series of materials that were not exposed to liquid nitrogen include both brittle materials (1.0036, 1.2767 and

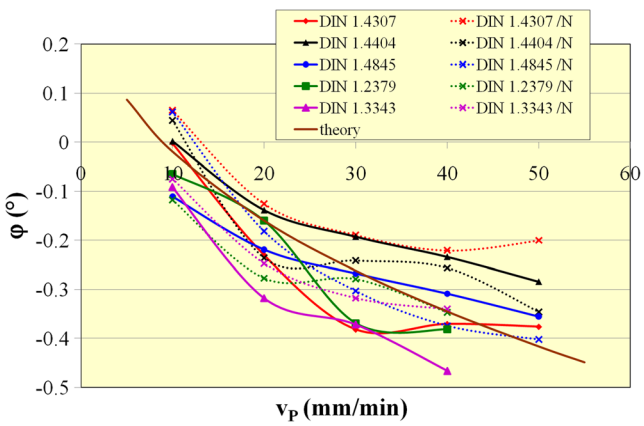

Fig. 5 Relation between the inclination angle of the cut walls made by AWJ and the traverse speed for cooled and non-cooled steels

1.7733), the curve of relation between traverse speed and inclination angle is precipitous; and ductile materials (1.3379 or 1.7225), their curve of relation between traverse speed and inclination angle is more gradual. The theoretical curve (Figs. 5 and 6), presented here as Eq. 11, was determined in [27] as an average line for steel samples with very different brittle/ductile behaviour.

5 Conclusions

The most important findings of presented research can be summarised in these points:

- Most of tested steels exhibit change in AWJ cutting characteristics induced by cooling to temperature of liquid nitrogen. Some of them became more resistant and ductile; other became less resistant and brittle.
- Differences between kerf widths measured on the inlet surfaces of samples prepared from selected steels are substantially lower than the ones determined on the outlet surfaces.
- The differences of kerf widths measured on the inlet surfaces of samples do not exceed uncertainties of the cutting process and measurement methods for selected steels.
- The differences of kerf widths measured on the outlet surfaces of samples exceed uncertainties of the cutting process and measurement methods, and they reflect the changes in material properties caused by cooling of selected steels to the temperature of the liquid nitrogen.
- The equation describing the relation between the traverse speed and the inclination angle of walls needs modification for higher thicknesses and steel plasticity.
- The ranges of difference between the inlet and the outlet width of kerf made by AWJ in tested steels are from 5.2 up to 35.4 % at the traverse speed of 5 mm min^{-1} and from 25.5 up to 44.9 % at the traverse speed of 50 mm min^{-1}.
- The ductile materials increase difference between the inlet and the outlet width of kerf made by AWJ at the traverse

speeds of 5 and 50 mm min^{-1} only up to 10 %, while the brittle and resistant to wear ones even over 35 %.

Acknowledgements The research presented in this paper was supported by International Visegrad Fund's Standard Grant No. 21220321 and by the project CZ.1.05/2.1.00/01.0040 "Regional Materials Science and Technology Centre—research activity New sources of strength and toughness of materials for high technological applications" within the frame of the operation program "Research and Development for Innovations" financed by the Structural Funds and from the state budget of the Czech Republic.

References

1. Hashish M (1989) A model for abrasive–waterjet (AWJ) machining. J Eng Mater Technol Trans ASME 111:154–162
2. Zeng J, Kim TJ (1996) An erosion model of polycrystalline ceramics in abrasive waterjet cutting. Wear 193:207–217
3. Kovacevic R, Yong Z (1996) Modelling of 3D abrasive waterjet machining: Part 1—theoretical basis. In: Gee C (ed) Jetting Technology. Mech. Eng. Pub. Ltd., Bury St Edmunds, pp 73–82
4. Yong Z, Kovacevic R (1996) Modelling of 3D abrasive waterjet machining: Part 2—simulation of machining. In: Gee C (ed) Jetting Technology. Mech. Eng. Pub. Ltd., Bury St Edmunds, pp 83–89
5. Hlaváč LM (1998) JETCUT - software for prediction of high-energy waterjet efficiency. In: Louis H (ed) Jetting Technology. Prof. Eng. Pub. Ltd., Bury St Edmunds, pp 25–37
6. Chen FL, Wang J, Lemma E, Siores E (2003) Striation formation mechanism on the jet cutting surface. J Mater Process Technol 141: 213–218
7. Henning A, Westkämper E (2006) Analysis of the cutting front in abrasive waterjet cutting. In: Longman P (ed) Water Jetting. BHR Group, Cranfield, pp 425–434
8. Monno M, Pellegrini G, Ravasio C (2006) An experimental investigation of the kerf realised by AWJ: the influence of the pressure fluctuations. In: Longman P (ed) Water Jetting. BHR Group, Cranfield, pp 309–321
9. Deam RT, Lemma E, Ahmed DH (2004) Modelling of the abrasive water jet cutting process. Wear 257:877–891. doi:10.1016/j. wear . 2004.04.002
10. Orbanic H, Junkar M (2008) Analysis of striation formation mechanism in abrasive water jet cutting. Wear 265:821–830. doi:10.1016/j. wear .2008.01.018
11. Hlaváč LM (2009) Investigation of the abrasive water jet trajectory curvature inside the kerf. J Mater Process Technol 209:4154–4161. doi:10.1016/j.jmatprotec.2008.10.009
12. Hloch S, Fabian S, Straka L (2006) Factor analysis and mathematical modelling of AWJ cutting. In: Kyttner R (ed) Proceedings of the 5th International Conference of DAAAM Baltic Industrial Engineering—Adding Innovation Capacity of Labour Force and Entrepreneur, Tallinn, Estonia, pp 127-132
13. Hloch S, Gombár M, Fabian S, Straka L (2006) Factor analysis of abrasive waterjet process factors influencing the cast aluminum surface roughness. In: Venkatesh VC, El-Tayeb NSM (eds) Proceedings of ICOMAST2006 International Conference on Manufacturing Science and Technology. GKH Press, Melaka, pp 145–149
14. Hlaváč L (1992) Physical description of high energy liquid jet interaction with material. In: Rakowski Z (ed) Geomechanics 91. Rotterdam, Balkema, pp 341–346
15. Hashish M (2004) Precision cutting of thick materials with AWJ. In: Gee C (ed) Water jetting. BHR Group, Cranfield, pp 33–45
16. Ma C, Deam RT (2006) A correlation for predicting the kerf profile from abrasive water jet cutting. Exp Thermal Fluid Sci 30:337–343. doi:10.1016/j.expthermflusci.2005.08.003
17. Shanmugam DK, Wang J, Liu H (2008) Minimisation of kerf tapers in abrasive waterjet machining of alumina ceramics using a compensation technique. Int J Mach Tools Manuf 48:1527–1534. doi:10.1016/j.ijmachtools.2008.07.001
18. Srinivasu DS, Axinte DA, Shipway PH, Folkes J (2009) Influence of kinematic operating parameters on kerf geometry in abrasive waterjet machining of silicon carbide ceramics. Int J Mach Tools Manuf 49: 1077–1088. doi:10.1016/j.ijmachtools.2009.07.007
19. Alberdi A, Rivero A, Lopez de Lacalle LN, Etxeberria I, Suarez A (2010) Effect of process parameter on the kerf geometry in abrasive water jet milling. Int J Adv Manuf Technol 51:467–480. doi:10.1007/s00170-010-2662-y
20. Wang JM, Gao N, Gong WJ (2010) Abrasive waterjet machining simulation by SPH method. Int J Adv Manuf Technol 50:227–234. doi:10.1007/s00170-010-2521-x
21. Hlaváč LM (1996) Interaction of grains with water jet—the base of the physical derivation of complex equation for jet cutting of rock materials. In: Gee C (ed) Jetting Technology. Mech. Eng. Pub. Ltd, Bury St Edmunds, pp 471–485
22. Hlaváč LM, Martinec P (1998) Almandine garnets as abrasive material in high-energy waterjet—physical modelling of interaction, experiment, and prediction. In: Louis H (ed) Jetting Technology. Prof. Eng. Pub. Ltd., Bury St Edmunds, pp 211–223
23. Hlaváč LM, Hlaváčová IM, Jandačka P, Zegzulka J, Viliamsová J, Vašek J, Mádr V (2010) Comminution of material particles by water jets—influence of the inner shape of the mixing chamber. Int J Miner Process 95:25–29. doi:10.1016/j.minpro.2010.03.003
24. Fabian S, Salokyová Š (2013) AWJ cutting: the technological head vibrations with different abrasive mass flow rates. Appl Mech Mater 308:1–6. doi:10.4028/www.scientific.net/AMM.308.1
25. Servátka M, Fabian S (2013) Experimental research and analysis of selected technological parameters on the roughness of steel area surface HARDOX 500 with thickness 40 mm cut by AWJ technology. Appl Mech Mater 308:13–18. doi:10.4028/www.scientific.net/AMM.308.13
26. Hlaváč LM, Strnadel B, Kaličinský J, Gembalová L (2012) The model of product distortion in AWJ cutting. Int J Adv Manuf Technol 62:157–166. doi:10.1007/s00170-011-3788-2
27. Hlaváč LM, Hlaváčová IM, Gembalová L, Jonšta P (2010) Experimental investigation of depth dependent kerf width in abrasive water jet cutting. In: Trieb FH (ed) Water Jetting. BHR Group, Cranfield, pp 459–467
28. Uhlář R, Hlaváč LM, Gembalová L, Jonšta P, Zuchnický O (2013) Abrasive water jet cutting of the steels samples cooled by liquid nitrogen. Appl Mech Mater 308:7–12. doi:10.1007/BF02649248
29. Strnadel B, Hlaváč LM, Gembalová L (2013) Effect of steel structure on the declination angle in AWJ cutting. Int J Mach Tools Manuf 64: 12–19. doi:10.1016/j.ijmachtools.2012.07.015
30. Paul S, Hoogstrate AM, van Luttervelt CA, Kals HJJ (1998) An experimental investigation of rectangular pocket milling with abrasive water jet. J Mater Process Technol 73:179–188. doi:10.1016/S0924-0136(97)00227-6
31. Paul S, Hoogstrate AM, van Luttervelt CA, Kals HJJ (1998) Analytical and experimental modeling of abrasive water jet cutting of ductile materials. J Mater Process Technol 73:189–199. doi:10.1016/S0924-0136(97)00228-8
32. Hashish M (1988) Visualization of the abrasive-waterjet cutting process. Exp Mech 28:159–169
33. Manu R, Babu NR, Ramesh N (2009) An erosion-based model for abrasive waterjet turning of ductile materials. Wear 266:1091–1097. doi:10.1016/j.wear.2009.02.008
34. Srinivas S, Babu NR (2012) Penetration ability of abrasive waterjets in cutting of aluminum–silicon carbide particulate metal matrix composites. Mach Sci Technol 16:337–354. doi:10.1080/10910344.2012.698935